The effect of thermo-catalytic reforming of a pyrolysis bio-oil on its performance in a micro-gas turbine burner

Mohsen Broumand [a], Muhammad Shahzeb Khan [a], Sean Yun [b], Zekai Hong [b], Murray J. Thomson [a],*

[a] Department of Mechanical and Industrial Engineering, University of Toronto, 5 King's College Road, M5S 3G8 Toronto, Ontario, Canada
[b] Aerospace Research Center, National Research Council of Canada, 1200 Montreal Road, K1A 0R6 Ottawa, Ontario, Canada

ARTICLE INFO

ABSTRACT

The combustion performance and pollutant emissions of a pyrolysis bio-oil (also called pyrolysis oil) upgraded with a thermo-catalytic reforming process were investigated experimentally in a micro-gas turbine burner and compared with those of a conventional bio-oil, ethanol (EtOH), and diesel fuel. The upgraded intermediate pyrolysis bio-oil called thermo-catalytic reforming bio-oil (TCRBO) has lower water and oxygen contents, suspended solid particulates, and non-volatile residue, along with higher carbon content, physical and chemical stability, and compatibility with fossil oils compared to the conventional fast pyrolysis bio-oil (FPBO). A stable flame with 100% TCRBO was possible in the present burner, whereas 50% by volume fraction EtOH had to be added to FPBO to improve its ignition and combustion characteristics. The original externally-mixed twin-fluid nozzle of the micro-gas turbine was replaced with an internally-mixed one which exhibited a superior performance with bio-oils. Over the practical range of air-to-liquid mass flow ratio for bio-oils, $0.3 < ALR < 0.7$, the spray Sauter mean diameter (SMD) of TCRBO was estimated larger than that of FPBO/EtOH blend for the both nozzles. However, most of the measured emissions from TCRBO spray flame were lower than those of FPBO/EtOH blend, owing to its improved combustion related properties, except nitrogen oxides (NO) which originated from the high nitrogen biomass feedstocks used for TCRBO production. Furthermore, contrary to FPBO, no flame instability due to the coke formation on the premixer tube of the burner was observed when using TCRBO. Conducting combustion investigations of the bio-oils in the present burner revealed that the thermo-catalytic reforming of bio-oil can greatly improve its ignition, combustion and pollutant emissions compared to conventional bio-oils.

1. Introduction

Because of concerns over the environment and sustainability, initiatives are increasingly taking place to replace fossil fuels using renewable carbon-neutral biofuels [1,2]. Biomass-derived pyrolysis oil (so-called bio-oil), is deemed a second-generation biofuel created from the thermal decomposition of biological wastes and residues such as wood chips, digestate, sewage sludge, etc., and is expected to be one of the most economically feasible renewable resources to facilitate the replacement of fossil oils in the near future [3,4]. This is on the grounds that the first-generation biofuels created from edible feedstocks (which have conflict with food production) have already been shown to be unsustainable moving forward [5], and the third- and fourth-generation biofuels currently have limited production scales due to their scarce biomass feedstocks and high production costs [6,7].

Bio-oils are generated from the thermal decomposition of biomass feedstocks in the absence of oxygen, called pyrolysis. In general, fast pyrolysis process produces higher liquid phase content of 70–80% (of dry biomass feedstock) than intermediate pyrolysis with liquid yields of 50wt%, which is in separate organic and water phases in the case of intermediate pyrolysis [8,9]. Despite lower liquid phase content, a wider range of biomass feedstocks with larger particle size, higher water content, and lower heat-transfer rate can be handled by intermediate pyrolysis due to its longer residence time in the reaction zone [8,9]. The fast pyrolysis process conditions for fast pyrolysis bio-oil (FPBO) generation from biomass are heating rates up to $500Ks^{-1}$, reaction temperatures between 673 and 823K, and vapor residence times of 0.5-2s [8,10]. Comparatively, thermo-catalytic reforming bio-oil (TCRBO) is generated through the combination of intermediate pyrolysis with the similar reaction temperatures as FPBO, but lower heating rates of 10-$100Ks^{-1}$ and longer reaction times of 240-600s, and a thermo-catalytic post-reforming process for improving the bio-oil quality [9,11].

In the post-reforming stage which occurs in a fixed bed reactor (see e.g., [12,13]), the char produced by the intermediate pyrolysis acts as a

---

catalyst at high temperatures, mostly in the range of 773–1023K [14], and its fixed carbon is stimulated through contacting with the pyrolyzed gases. This improves the water–gas shift reactions and enhances the secondary cracking reactions of pyrolysis products. Leaving the post-reformer, the vapors are quenched in a series of condensers with temperatures below 273K and the liquid phase is separated by gravity [12,13]. Applying the post-reforming process reduces the overall liquid yields of intermediate pyrolysis from 50wt% to 27-37wt% with an organic phase (which is called TCRBO) of 6-11wt% [9]. Notwithstanding the smaller liquid yields of TCRBO compared to FPBO, which might affect its production scales and costs, its improved combustion related properties, such as lower water and oxygen contents, suspended solid particulates, and non-volatile residue, along with higher carbon content, chemical and physical stability, and compatibility with fossil oils [9], are expected to make TCRBO more compatible with the existing combustion systems.

Bio-oils have the potential to be used in burners, boilers, and furnaces, as well as gas turbine and compression-ignition engines [1,15,16]. For power generation in a distributed manner, interest in micro-gas turbines (power output <500kW) is growing due to its high combustion efficiency and durability, and low harmful emissions, noise, and maintenance costs. More importantly, micro-gas turbines have the ability to combust liquid biofuels with less favorable/refined properties [17]. One of the most widespread commercial micro-gas turbines in recent years is the Capstone C30 (30kW) [18–21] with the potential to be used as an automotive range extender in hybrid electrical vehicles or a decentralized unit for heat and power supply in rural areas. The C30 engine has an annular design in which three burners are tangentially aligned and generate cyclonic flow inside the combustion chamber [21]. The burners work based on a Lean Premixed Prevaporized (LPP) combustion where the liquid fuel is injected inside a premixer tube with an externally-mixed twin-fluid nozzle and premixes with primary combustion air before combustion [22,23]. A detailed experimental information on the operational behavior and cycle parameters of a C30 micro-gas turbine running on a conventional gas turbine fuel (i.e., Jet-A1 kerosene) is reported in [20].

There exist several studies in the available literature which evaluated the effect of renewable liquid fuels on the performance and emissions of the Capstone C30. For a C30 system running on soybean oil derived methyl ester, higher carbon monoxide (CO) and nitrogen oxides (NO_X) emissions were reported for the biodiesel compared to those of No. 2 diesel fuel [24,25]. In another study conducted by Brookhaven National Laboratory [26], both CO and NO_X emissions slightly decreased when replacing No. 2 heating oil with soy oil biodiesel under full load operation. A series of other experiments on castor biodiesel showed that CO and NO_X increased and decreased, respectively, when replacing diesel fuel with the preheated castor biodiesel in C30 [27]. One study used straight vegetable sunflower oil in C30 and reported the same CO emissions for the preheated vegetable oil at the nominal condition as for diesel fuel, and higher NO_X emissions were observed for the preheated vegetable oil, which was correlated with its fuel-bound nitrogen [28]. In another study using JetA1 blended with 20% (by volume) of rapeseed oil or sunflower oil, no change in the concertation of gaseous emissions compared to neat JetA1 was observed [29]. However, they demonstrated that particulate matter (PM) emission increased about three times and more than fifty times for the blends of rapeseed oil and sunflower oil, respectively, compared to that of Jet A1.

Because the studies on real Capstone C30 micro-gas turbine engines have reported different emission trends with alternative fuels, developing a dedicated burner test rig to reproduce the geometry and conditions present in the original burner of the C30 is required to better observe the flame and to more easily locate the diagnostics. In this regard, one study conducted a series of experiments with and without the premixer tube of the C30 injector in a laboratory test rig to isolate the effect of this section on the emissions of No. 2 diesel fuel [22]. In addition to the fuel atomization and evaporation effects, they highlighted the importance of the fuel/air mixture properties (e.g., the temporal and spatial distribution of homogeneity) on the exhaust emissions in the early stages of the combustion. Another study constructed a burner similar to the real burner of the C30 with a spray flame in a non-enclosed environment [30]. Using preheated rapeseed oil and superheated steam instead of air (for hindering the near-nozzle fuel polymerization during its atomization), they reported equal CO and 60% lower NO_X emissions compared to diesel fuel.

While using bio-oils in micro-gas turbines for heat and power generation purposes has great environmental and techno-economic benefits, the difficulties in atomization and combustion of conventional bio-oils like FPBO in small-scale combustion systems have caused different challenges such as high PM emissions and coke deposition, which are mainly attributed to the unique physicochemical properties of FPBO. These include high viscosity, water and oxygen contents, solid content, non-volatile residue, and physical and chemical instabilities, along with low energy density and incompatibility with conventional fossil oils [1,15]. The spray combustion of conventional bio-oils like FPBO begins with evaporation and combustion of low-molecular-weight volatile components, along with the thermal cracking and gasification of high-molecular-weight components. This is followed by the combustion of the components with low volatility and finally the burnout of non-volatile components [31–33]. The residual non-volatile components in the last stage are responsible for coke deposition, char formation and PM emissions if burnout within the combustion region is incomplete. Therefore, using FPBO in small-scale applications which require the fuel to be fully evaporated within a short time frame and small volume is more challenging than in large-scale combustors.

The goal of the present study is, therefore, to facilitate and optimize the combustion performance and emissions of bio-oils in a C30 micro-gas turbine burner by adopting two strategies. The original externally-mixed twin-fluid nozzle of C30 was, first, replaced with an internally-mixed twin-fluid nozzle which exhibited a superior performance with the atomization of highly viscous liquids like FPBO which have high solid content and coking propensity [33]. Then, an upgraded bio-oil, called TCRBO, with higher distillability (less residue) than FPBO have been examined to reduce the non-volatile components which have slow surface combustion in the last stage; this improves the combustion performance and emissions of bio-oils. In the end, the performance and gaseous and PM emissions of the two different bio-oils were compared with those of diesel fuel to examine the practicality of the displacement of fossil oils in C30 Capstone micro-gas turbines. To the best of the authors knowledge, no study was reported in the available literature on the successful deployment of a pure (100%) pyrolysis bio-oil in a C30 micro-gas turbine, which would facilitate the further deployment of renewable liquid biofuels in biopower systems. The present study is the first published combustion study of TCRBO in a gas turbine burner.

2. Experimental detail

2.1. Bio-oils properties

Two different types of available biomass-derived pyrolysis oils, FPBO extracted from white softwood residue [34,35] and TCRBO from sewage sludge [36,37], are used in the present study. The properties of theses bio-oils along with the test method employed for their estimations are introduced and compared with those of EtOH and No. 2 diesel fuel in Table 1. In addition to the compositions of biomass feedstocks and production process, the post-production (upgrading) process, such as the thermo-catalytic reforming of TCRBO in the present study, can significantly improve the physicochemical properties of a bio-oil. In comparison with FPBO, TCRBO has a higher carbon content and therefore a greater lower heating value (LHV), which is close to that of No. 2 diesel fuel. TCRBO's lower oxygen and water contents are the other important distinctions between the bio-oils, making it miscible in fossil oils

Table 1
Fuel property summary and comparative chart.

Parameter	Unit	Test Method	EtOH	FPBO	TCRBO	No. 2 Diesel Fuel [a]
Density	kg/m^3 at 20°C	EN ISO 12185, ASTM D4052	789	1256	1014	830 - 860
Surface Tension[b]	N/m at 25°C	-	21.97×10^{-3}	34×10^{-3}	28.5×10^{-3}	28×10^{-3}
Kinematic Viscosity	m^2/s at 25°C	EN ISO 3104, ASTM D445	1.36×10^{-6}	81×10^{-6}	87×10^{-6}	2×10^{-6} - 6×10^{-6}
C-H-O-N	wt%, dry	ASTM D5291	52.14-13.12-34.7-(-)	45.79-7.11-47.10-0.00	77.4-7.7-4.5-9.6	87-13-0-(<0.01)
Sulfur Content	wt%, dry	EN ISO 20846, ASTM D5453	0	<0.05	0.8	0.1
Water Content	wt%	ASTM E203	7.2	15 – 30	1.7	0.0
Solid Content	wt%	ASTM D7579	0	<1	<0.1	-
Ash Content	wt%	EN ISO 6245	0	<0.3	<0.05	<0.001
TGA residue	wt%	-	0	20	3	0
LHV	MJ/kg	DIN51900, ASTM D240, ASTM D5291 for H	26.9	16.9	34.0	41- 43
Acidity[a]	pH	ASTM E70	7	2 – 3 TAN=70-100 (mg$_{KOH}$/g)	TAN=4.6 (mg$_{KOH}$/g)	7

[a] Typical ranges from literature [1,15,38]

[b] Measured using a Fischer Scientific (Ottawa, ON) Manual Model 20 Surface Tensiometer.
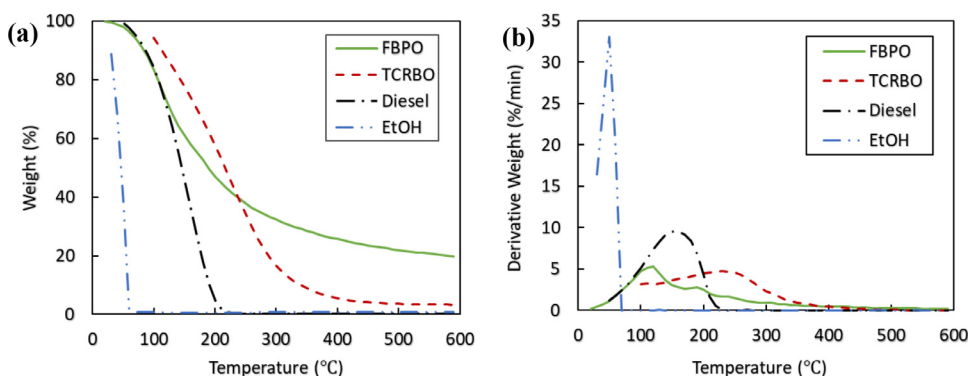
Fig. 1. (a) Thermogravimetric analysis (TGA) and **(b)** differential thermogravimetric analysis (DTGA) curves for the fuels in Table 1.

contrary to FPBO. The higher oxygen content of FPBO is responsible for its lower LHV, higher corrosivity, acidity, and chemical instability (i.e. aging) [1,9]. The FPBO's higher water content also leads to flame instabilities as it results in a low LHV, delayed ignition from slow vaporization, and reduced flame temperatures and combustion rates (due to the high thermal capacity of water) [1,9]. The higher suspended solid contents within FPBO, which is composed of inorganic ash and organic char (known as primary char), increases its hazardous pollutants in the form of PM emissions. The density, viscosity, and surface tension of both the bio-oils, which are important for fuel atomization, are in the same ranges, while their viscosities are much larger than that of No. 2 diesel fuel.

Thermogravimetric analysis (TGA) tests were performed by heating 20mg of fuel up to 600°C under an inert atmosphere of nitrogen at a rate of 10°C/min for estimating the non-volatile residue of the fuels in Table 1. The distillation behavior of the fuels is depicted in Fig. 1a. While EtOH and diesel are fully evaporated (<1wt%) at a temperature of about 70°C and 200°C, respectively, FPBO and TCRBO do not reach a zero sample weight percent even at 600°C, with a much lower non-volatile residue for TCRBO with 3wt% (of the original sample) compared to 20wt% for FPBO. This indicates that FPBO is more susceptible to fuel coking, heterogeneous solid-phase combustion, and PM emissions [1]. The differential thermogravimetric analysis (DTGA) curves in Fig. 1b show that the major weight loss rates for FPBO and TCRBO occur at 120°C and 230°C, respectively, with about 5%/min. The peak loss rates of EtOH and diesel are 7 and 2 times higher than those of the bio-oils occurring at 50°C and 150°C, respectively.

2.2. Experimental setup and diagnostics

A model burner installed in an enclosed double-insulated 10kW combustion chamber (Fig. 2a), a nozzle with fuel injection system, and several diagnostic systems comprised the main components of the experimental setup in the present study. The burner was designed and constructed to represent one of the three burners of a C30 Capstone microgas turbine and consisted of a cylindrical enclosure, a twin-fluid nozzle, and a premixer tube illustrated in Fig. 2b. The combustion air distribution inside the combustion chamber was adjusted to prevent flame instabilities and blow out at the burner section. In doing so, one-third of the overall combustion air passed through the premixer tube as a primary combustion air and the rest of the air (secondary air) was injected equally into the chamber through the three separate holes placed on its port box, see Fig. 2a. The primary combustion air was pulled downwards with a negative pressure stack fan and, after being preheated to about 140°C, was symmetrically distributed in the cylindrical enclosure with passing through a swirl box with swirl number of zero (i.e., co-flow). The diameter of the cylindrical enclosure was 100mm and inserted 200mm into the combustor throat to have a direct visualization of the flame from its quartz viewports. The closed bottom-side of the enclosure was machined to make a circular hole with a step to allow the premixer tube to sit on and introduce the fuel/air mixture into the combustion chamber, see Fig. 2b. The nozzle was centered downwardly through the enclosure and connected to the premixer tube using a designed adaptor. The fuel was preheated up to 80°C by the surrounding primary air with high temperature, as the nozzle passed through the swirl box and enclosure
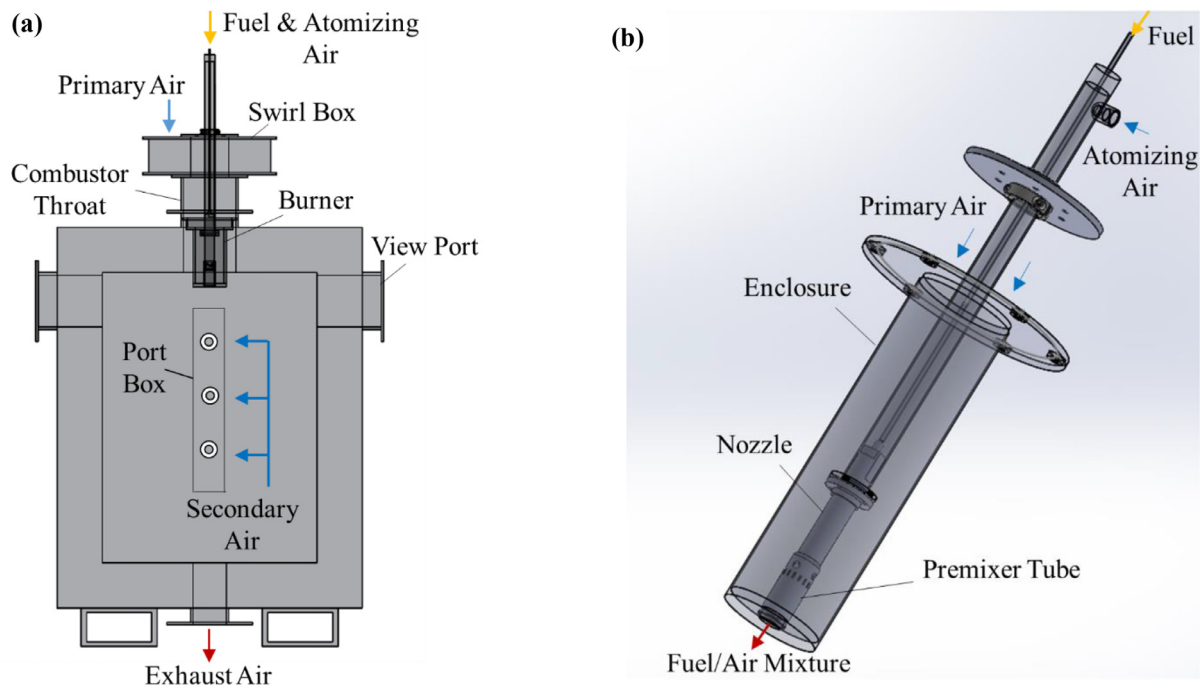
Fig. 2. Schematic view of **(a)** combustion chamber and **(b)** burner section.
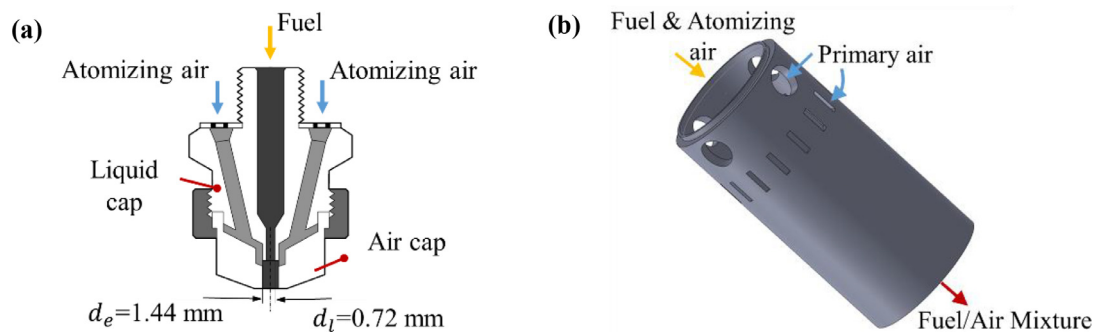

Fig. 3. Schematic diagram of **(a)** internally-mixed twin-fluid nozzle and **(b)** premixer tube.

sections, which decreased the fuel viscosity and subsequently improved its atomization.

The fuel injector designed for the present study was the same as the nozzle/premixer assembly used in a C30 Capstone micro-gas turbine [25]. The original C30 externally-mixed twin-fluid nozzle was replaced with a single hole internally-mixed twin-fluid nozzle with the same equivalent exit diameter of d_e=1.44mm (Fig. 3a) [34]. The liquid fuels were delivered to the nozzle using a peristaltic pump and its flow rate was set to provide the burner with a fuel energy input of 10kW. The premixer tube was adopted from the original C30 micro-gas turbine injector with a length of 55mm and diameter of 26mm. It consisted of four orifices with diameter of 8mm for the introduction of primary air into the premixer tube and a helical swirler with dimensions of 1mm × 9mm for enhancing the spray droplet evaporation and fuel/air mixing before combustion, see Fig. 3b.

A zirconia (ZrO2) model OXY6200 oxygen sensor was used to continuously monitor the oxygen percentage in the exhaust. Gaseous pollutants, such as CO and nitric oxide (NO) concentrations were measured using Nicolet 380 Fourier transform infrared spectroscopy (FTIR). The amount of unburned hydrocarbon (UHC) in the exhaust was estimated using a flame ionization detector (FID). The UHC emissions were measured as parts per million (ppm) of methane with an uncertainty of ±3 ppm. PM measurement and analysis were carried out according to the

isokinetic particulate sampling method. While the burner was running at a steady operating condition, two consecutive filters were used to collect PM samples. After drying the filters at a temperature of 150°C in an oven for 2h, carbonaceous residue (CR) was estimated by burning off the carbon from the filters in the oven post-combustion at a temperature of 750°C for 1h and measuring the filter mass before and afterwards (based on ASTM D4422). Full details of the diagnostics and PM measurements along with the uncertainty of the devices are available elsewhere [34].

2.3. Experimental conditions and procedures

The flow rates of the fuels were changed between 17 and 29mL/min (according to the fuels' LHV in Table 1) to provide the combustor with a fuel energy input of 10kW. Accordingly, the atomizing airflow rates were changed between 8 and 12L/min to approximately reach a same range of air-to-liquid mass flow ratio (ALR= $\dot{m}_a/\dot{m}_l$) at all the test conditions. A 0.34kW CH_4/O_2 pilot flame was used for fuel ignition and to stabilize the spray flame during operation. Considering the primary combustion air flow rate which was 100L/min and the secondary air at about 165-185L/min, the atomizing air flow rate, and the pilot flame, the combustor could reach its efficient operating condition with an equivalence ratio between 0.51and 0.53, or 89-96% excess air and 9.2-9.6% O_2 in the exhaust, according to the detailed experimental information on the

Table 2
Conditions used for combustion testing.

Case #	Fuel	Fuel flow (mL/min)	Atomizing air flow (L/min)	ALR ($\dot{m}_a/\dot{m}_l$)
1	EtOH	29	12	0.65
2	Diesel	17	8	0.7
3	TCRBO	18	10	0.67
4	FPBO50	26	12	0.53

same chamber [34]. The equivalence ratio was also back-calculated assuming that complete combustion takes place using measured O_2 in the exhaust. The smaller stoichiometric mass air-to-fuel ratio (AFR) of bio-oils compared to that of diesel fuel compensates for their lower LHV (see Table 1). Nonetheless, to maintain a given thermal energy release rate with complete combustion, the bio-oils require 10-20% more combustion air than diesel fuel as their LHV/LHV_{diesel} is slightly smaller than their AFR/AFR_{diesel}.

For each bio-oil the combustion chamber was first warmed up with EtOH for about 30min, the EtOH emissions measurements were taken, and then it ran on diesel for another 30min before taking the diesel measurements. After that, the combustor was again switched to EtOH and ran for another 15min to clean the fuel line and nozzle, and finally ran on one bio-oil for about 30min until the exhaust temperature was above 250°C, with the presence of primary air heating. At this point, while the sufficiently warm double-insulated combustor facilitated the spray flame stability, the bio-oil emissions measurements were taken. After that, the combustor was again flushed with EtOH and the same procedure was repeated for the other bio-oil. During the preliminary tests using 100% FPBO, no stable flame was achieved because of the impingement of FPBO spray droplets on the inner wall of the burner premixer tube. To address this issue, 50% (by volume) of EtOH was added to FPBO (FPBO50) to improve the fuel's volatility and therefore to reduce its coke formation rate. The preliminary tests also showed that at very low values of ALR, bio-oils were not atomized properly and large unevaporated droplets impinged and dripped out of the tube, began to coke and grow on the high-temperature edge of the tube and finally extinguished the flame. On the other hand, when the atomizing airflow was increased too much, the flame began to oscillate due to shear forces inside the premixer tube, ultimately blowing out if the air continued to increase. Both limits resulted in a narrow practical range of 0.3 < ALR < 0.7 in the present experimental setup and emphasizing the role of an effective atomization in the efficient combustion of bio-oil sprays. In this regard, the combustion test conditions for the most stable flame of different fuels are listed in Table 2.

3. Results and discussion

3.1. Spray characteristics of bio-oils

The spray formation process (i.e., atomization) plays an important role in ignition and combustion of liquid fuels [39,40]. More importantly, during the combustion of bio-oils, having an effective atomization can accelerate the evaporation of the fuel by generating small droplets and optimize their heating rate in a combustor by increasing their hot-zone residence times [1,33]. This can minimize the amount of the solid residues (known as secondary char) formed during FPBO droplet combustion. This is supported by the fact that the size of the residues is comparable to that of the original size of fuel droplets [15,41]. Therefore, in the present designed burner, the original C30 externally-mixed twin-fluid nozzle was replaced with the internally-mixed one to exploit its rapid disruption of the liquid stream and generate bio-oil sprays with smaller droplets. This is on the grounds that an internally-mixed twin-fluid nozzle features the prompt atomization mechanism and is less sensitive to liquid's properties, particularly viscosity, in comparison with the classical atomization mechanism presented in an externally-mixed nozzle [39,40]. Moreover, internally-mixed twin-

fluid nozzle has a larger liquid line which can prevent the clogging of the nozzle by the solid particles of bio-oils and reduce the coke formation rates on the nozzle's tip during operation [34]. To show the effects of fuel properties and nozzle types (or atomization mechanisms) on the spray SMD of the fuels, two empirical correlations for the classical atomization proposed by Varga et. al. [42], Eq. (1), and prompt atomization by Lefebvre [43], Eq. (2), were used as follows:

$$SMD_E = \frac{0.68A^{1/2}\left(\rho_l v_a\right)^{1/4}\sigma^{1/2}}{\rho_a^{3/4}\left[u_a\left(1+\sqrt{\rho_a/\rho_l}\right)-u_l\right]u_a^{1/4}} \tag{1}$$

$$SMD_I = \frac{3}{2/d_l + B\rho_l u_a^2/\left[4\sigma(1+1/ALR)\right]} \tag{2}$$

where ρ_a and v_a is the air density and kinematic viscosity, and ρ_l and σ are the liquid density and surface tension, respectively. u_a and u_l are the atomizing air velocity and liquid velocity at the nozzle exit, and A=0.055m^2 and B=0.007 are constants. d_l=0.4 and 0.72mm are the liquid-stream exit diameters for the externally- and internally-mixed nozzles, respectively, and the air-stream exit diameters for the both nozzles were considered to be close to d_e=1.44mm.

The kinematic viscosities of bio-oils were measured at different temperatures and compared with that of diesel fuel in Fig. 4a. The values of 100% FPBO is shown for comparison. As is shown in this figure, the viscosity of TCRBO and 100% FPBO decreased asymptotically with increasing the temperature and reached close to that of the diesel fuel at 80°C, while adding 50% (by volume) EtOH to FPBO had approximately similar effect on the viscosity of FPBO50 and made the viscosity of the fuel blend close to that of the diesel. The effect of temperature on the surface tension and density of the liquid fuels were neglected and their values at 25°C were used to find the spray SMD of bio-oils [38]. Fig. 4b depicts the spray SMD of the fuels injected from the two nozzles at various ALRs, which are estimated from Eqs. (1) and (2). As was expected, the spray SMD decreased and generally displayed asymptotic behavior beyond a certain point with increasing ALR [39,40]. At sufficiently high ALRs (e.g., 0.5<ALR), the SMD of the spray droplets generated by the internally-mixed nozzle was estimated to be smaller than that of the externally-mixed one by approximately 50%, which is beneficial in the spray combustion of bio-oils as small droplets reduce the combustion emissions and coke formation rates of the bio-oil. For the both nozzles, while the SMD of the bio-oils are smaller than that of the diesel fuel, the estimated SMD of the FPBO/EtOH blend was smaller than that of TCRBO due to the higher atomizing air velocity (u_a) of the FPBO/EtOH blend at each specific ALR.

3.2. Combustion characteristics of bio-oils

Fig. 5 shows the spray flames of the fuels and conditions of Table 2 using the internally-mixed nozzle in the present C30 micro-gas turbine burner. Contrary to 100% FPBO, TCRBO exhibited a stable flame owing to its higher carbon content and lower oxygen and water contents, which facilitated its ignition and combustion, along with its higher distillability which reduced the fuel polymerization and coke formation rates on the premixer tube of the burner. According to the observations, while the flame was stable for EtOH, Diesel, and TCRBO, it became highly unstable with FPBO and ultimately extinguished because of the impingement and polymerization of FPBO on the high-temperature
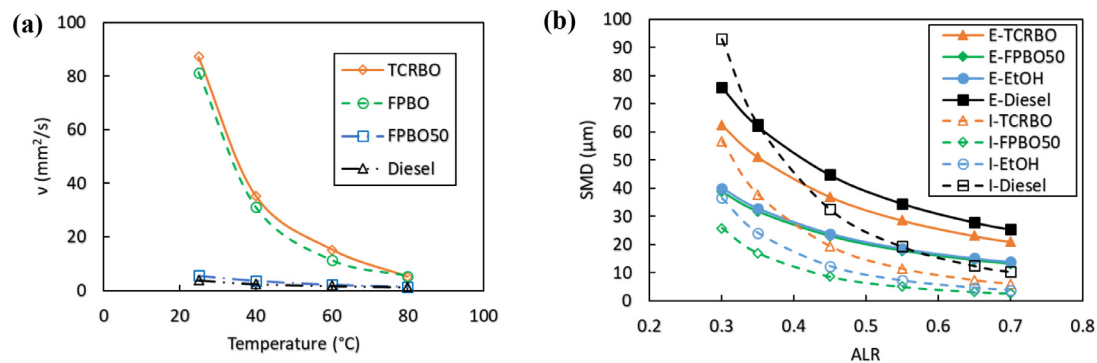
Fig. 4. Variation of **(a)** kinematic viscosity of bio-oils versus temperature and **(b)** spray SMD versus ALR for the bio-oils at 80°C and EtOH and diesel fuel at room temperature.
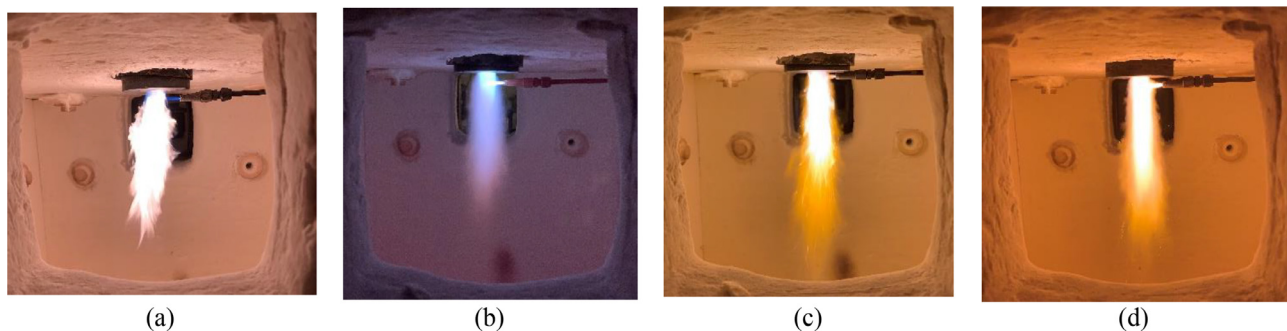

Fig. 5. Spray flames of **(a)** Diesel, **(b)** EtOH, **(c)** TCRBO, and **(d)** FPBO50.

inner wall of the burner premixer tube, which produced a layer of fuel coking on its surface and blocked the small swirler slits of the tube. That degraded the droplet evaporation and fuel/air premixing inside the tube and the flame was finally extinguished with the rapid growth of coke layers inside the tube. To have a stable FPBO flame, a blend of 50/50 (by volume) of FPBO/EtOH was used to ameliorate the fuel's volatility and subsequently lower its non-volatile residue from 20wt% (Table 1) to 13wt%. As is depicted in this figure (see also videos in Supplemental Materials), diesel fuel and EtOH (Fig. 5a and 5b) burned homogeneously due to the quick evaporation of their droplets, whereas for TCRBO and FPBO50 (Fig. 5c and 5d), in addition to the combustion of volatiles in the near-nozzle (bright core) region, char burning (through surface heterogeneous combustion) was evident in the far-field region.

It should be mentioned that it was impossible to increase the FPBO volume fraction more than 50% in the FPBP/EtOH blend in the present burner and using the internally-mixed nozzle, as it caused a similar coking and flame extinguishing problems due to the elimination of the dilution influence of EtOH. In fact, contrary to the TCRBO and FPBO50 tests where no significant fuel residue built-up was observed on the inner wall of the tube at the end of their combustion tests, a large amount of coke was formed during the FPBO75 (75/25 FPBO/EtOH) test, particularly on the upper half of the tube close to its swirler slits and nozzle exit. The images of the burner premixer tubes after the combustion tests of FPBO50 and FPBO75 blends are shown in Fig. 6.

3.2.1. Gas-phase emissions

During the spray combustion of bio-oils, UHC emissions closely follow the CO emissions and both are sensitive to the test conditions, such as ALR when using twin-fluid nozzles, whereas the important mechanism for NO emissions is attributed to the conversion of fuel-bound nitrogen [31,44]. In essence, while the thermal NO (formed by Zeldovich Mechanism [45]) is very temperature dependant, NO emissions from fuel-bound nitrogen (formed by Fenimore Mechanism [46]) is relatively insensitive to temperature and correlated with the nitrogen contents of
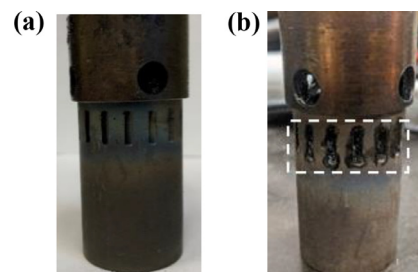

Fig. 6. Images of the premixer tubes after **(a)** FPBO50 and **(b)** FPBO75 combustion tests, where the rectangle indicates the locations of the formed coke.

the biomass feedstocks used for producing the bio-oils. In addition to the test conditions with flame instabilities and local extinctions, CO can also be formed during the last stage of bio-oil spray combustion where the char particles are burning in a relatively lower temperature environment of the combustor [1].

Fig. 7a compares the levels of CO, UHC and NO emissions in the exhaust gases of the combustion chamber for the test conditions in Table 2. Regarding the bio-oils emissions, CO and UHC concentrations of TCRBO are much lower than those of FPBO50, which is attributed to the improved combustion related properties of TCRBO, such as higher carbon content and lower oxygen and water contents, which facilitate its ignition and combustion in the present burner. However, the NO emissions of TCRBO is more than ten times higher than those of FPBO50. This is mainly attributed to the higher nitrogen content of TCRBO used in the present study (Table 1), which originates from its biomass feedstocks (i.e., sewage sludge), whereas FPBO which is derived from white softwood residue which has much lower nitrogen content. As is depicted in this figure, NO and UHC of EtOH and diesel fuel have the lowest values with both having approximately the same CO of 15ppm. Overall, the other gaseous emissions associated with the bio-oils are higher than
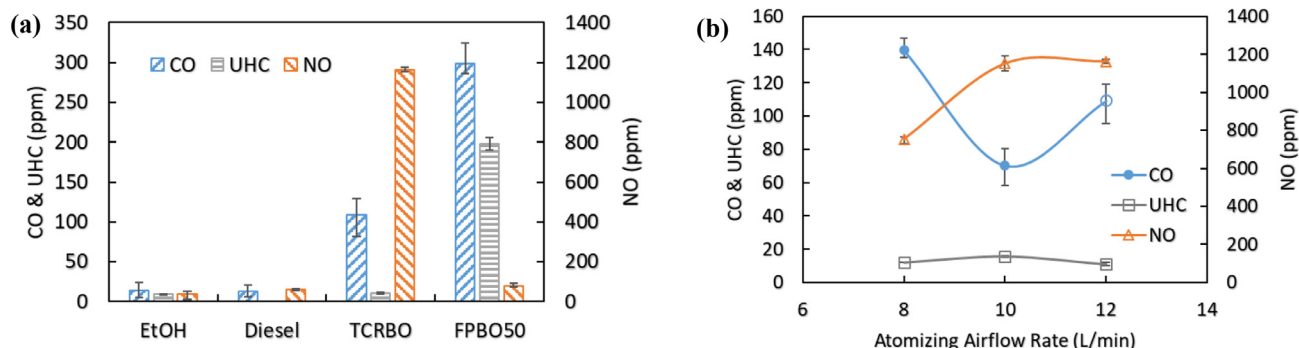
Fig. 7. Comparison of the gaseous emissions of **(a)** the test conditions in Table 2 and **(b)** TCRBO at different atomizing airflow rates.
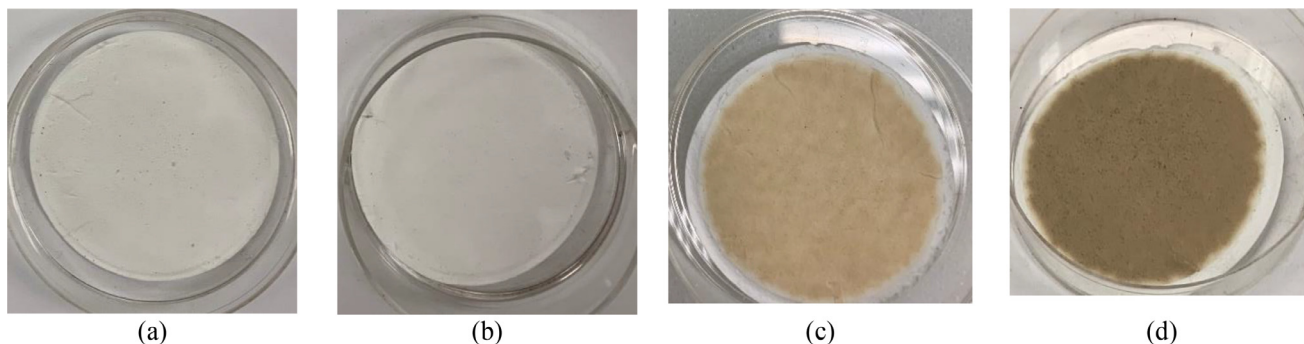

Fig. 8. Images of PM deposition on filters for **(a)** Diesel, **(b)** EtOH, **(c)** TCRBO, and **(d)** FPBO50.

EtOH and diesel; exceptions are the UHC emissions of TCRBO which is close to that of EtOH and the NO concentrations of FPBO which is in the same range as for diesel. This is mainly because of the combustion related properties of bio-oils (Table 2) which degrade the fuel evaporation and fuel/air mixing compared to EtOH or diesel, increasing the coking tendency and flame instabilities of the bio-oils. It is also noteworthy that the emissions of the diesel fuel in the present study were approximately in the same range as the exhaust gas emissions of the real Capstone C30 micro-gas turbine when running on Jet-A1 kerosene using one burner [20], though the operating conditions and combustor geometries are different in the two studies.

Because of the better combustion performance of TCRBO compared to FPBO in the present burner, a study was performed to optimize the combustion conditions of TCRBO by examining the effects of the atomizing air flow rate (or ALR) on its emissions. Hence, atomizing air flow rate was changed in the range in which the TCRBO flame was found to be well stabilized (i.e., between 8 and 12 L/min) for emission measurements shown in Fig. 7b. The emission trends in this image can be well explained by considering the effect of atomization on the combustion performance and emissions of bio-oils. With increasing the atomizing airflow from 8 to 10 L/min, the smaller droplets (SMD) of the TCRBO spray at higher ALRs undergo a faster and more thorough burnout, consuming CO and increase the flame temperature or thermal NO. However, opposite emission trends were observed with further increasing the atomizing airflow from 10 to 12 L/min, resulted from the higher near-nozzle shear-forces at high ALRs. These excess shears impose flame instabilities, reduce the hot-zone residence times of the droplets, and finally cause flame lift-off or blow-out; all of which increase CO and slightly decrease NO in the exhaust due to incomplete combustion.

3.2.2. Solid-phase emissions

Fig. 8 shows the images of PM deposition on the filters for the fuels and test conditions in Table 2. Concerning the solid-phase emissions of the bio-oils, the filters of FPBO50 and TCRBO are covered in a matte black powder which is indicative of unburned CR. However,
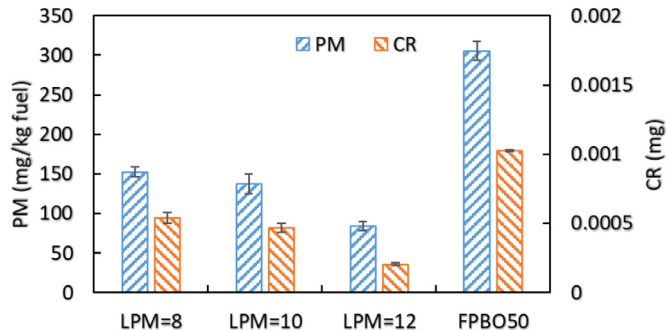

Fig. 9. Comparison of the total PM and CR emissions of TCRBO at different atomizing airflow rates and FPBO50.

the brighter filter of TCRBO is another factor (in addition to the gaseous emissions) which shows the better combustion performance of TCRBO in the present burner. This is specifically due to the lower ash, solid content and non-volatile residue of TCRBO compared to those of FPBO (see Table 1). The suspended solids within a bio-oil are composed of inorganic ash and organic char (or primary char) which are important contributions to PM emissions. In addition, the polymerization inside the bio-oil droplets during their flight in a combustor (or secondary char) which is correlated with the non-volatile residue of the bio-oil, and droplet sizes and their heating rates can increase the overall PM emissions [1]. As was expected, the measured PM emissions of the diesel and EtOH were negligible in comparison with those of the bio-oils.

Fig. 9 depicts the levels of CR and total PM in the exhaust gases of the combustor for the stable test conditions of bio-oils, TCRBO (Fig. 7b) and FPBO50 (Table 2). Comparing the results shows that both the CR and PM of FPBO50 are more than twice of those of TCRBO which are consistent with the qualitative observations of the CR deposition on filter images in Fig. 8c and 8d. In addition to smaller CR amount, the lower ash content of TCRBO compared to that of FPBO (Table 1) is another

contributing factor to the smaller total PM of TCRBO. Since PM consists of partially burned CR and ash, the gradual decrease in the amounts of CR and accordingly total PM of TCRBO (as its ash content is constant) with increasing the atomizing airflow rate also shows the role of atomization in the secondary char particles formation and burnout.

4. Conclusion

Gaseous and particulate matter emissions of two pyrolysis oils extracted from different biomass feedstocks and production processes are experimentally investigated in a micro-gas turbine burner. The properties of bio-oils directly affect the combustion performance and emissions of the flames by influencing the fuel atomization, evaporation, fuel/air mixing, and ignition characteristics. Adding 50% (by volume) EtOH to FPBO ameliorates the fuel viscosity and volatility which subsequently improves its atomization and ignition characteristics, reduces the coke formation rates inside the burner premixer tube, and finally sustains the stability of its spray flame during experiments. Because adding EtOH, as a first-generation biofuel created from edible feedstocks, to a crude bio-oil (like FPBO) is not considered to be a sustainable approach in the future, a bio-oil with upgraded properties, such as TCRBO with lower pollutant emissions, is preferable for using in a micro-gas turbine engine. The higher physical and chemical stability of TCRBO [9] compared to FPBO also facilitates its long-term storage, though the stability characteristics of the bio-oils require further analyses. Nonetheless, the lower liquid production yields and higher costs of such upgraded bio-oils could limit their widespread utilization, necessitating a techno-economic analysis and life cycle assessment on them. Regarding the superior combustion performance of TCRBO compared to FPBO in the present C30 burner, it can be concluded that, while the carbon, water and oxygen contents of a bio-oil are known to be the predominantly controlling parameters of its combustion, the role of bio-oil's non-volatile residue in the coke formation and growth inside the burner premixer tube, as well as its impacts on the formation and burnout of char particles in the combustor should not be overlooked. Finally, because the TCRBO used in the present study was extracted from sewage sludge, which has high nitrogen contents, the use of a TCRBO from other biomass feedstocks with lower nitrogen, such as woody residues, or applying the thermo-catalytic post-reforming process on a wood-derived fast pyrolysis bio-oil would be helpful for having a high quality bio-oil with reduced nitrogen content and non-volatile residues.

Declaration of Competing Interest

The authors declare that they have no known competing financial interests or personal relationships that could have appeared to influence the work reported in this paper.

Acknowledgments

Supplementary materials

Supplementary material associated with this article can be found, in the online version, at doi:10.1016/j.jaecs.2020.100017.

References

[1] Broumand M, Albert-Green S, Yun S, Hong Z, Thomson MJ. Spray combustion of fast pyrolysis bio-oils: applications, challenges, and potential solutions. Prog Energy Combust Sci 2020;79:100834.

[2] Seljak T, Buffi M, Valera-Medina A, Chong CT, Chiaramonti D, Katrašnik T. Bioliquids and their use in power generation – a technology review. Renew Sustain Energy Rev 2020;129:109930. 10.1016/j.rser.2020.109930.

[3] Elliott DC, Meier D, Oasmaa A, van de Beld B, Bridgwater AV, Marklund M. Results of the international energy agency round robin on fast pyrolysis bio-oil production. Energy Fuels 2017;31:5111–19. doi:10.1021/acs.energyfuels.6b03502.

[4] Meier D, van de Beld B, Bridgwater AV, Elliott DC, Oasmaa A, Preto F. State-of-the-art of fast pyrolysis in IEA bioenergy member countries. Renew Sustain Energy Rev 2013;20:619–41. 10.1016/j.rser.2012.11.061.

[5] Sims REH, Mabee W, Saddler JN, Taylor M. An overview of second generation biofuel technologies. Bioresour Technol 2010;101:1570–80. 10.1016/j.biortech.2009.11.046.

[6] Leong W-H, Lim J-W, Lam M-K, Uemura Y, Ho Y-C. Third generation biofuels: a nutritional perspective in enhancing microbial lipid production. Renew Sustain Energy Rev 2018;91:950–61. 10.1016/j.rser.2018.04.066.

[7] Abdullah B, Syed Muhammad SAF, Shokravi Z, Ismail S, Kassim KA, Mahmood AN, et al. Fourth generation biofuel: a review on risks and mitigation strategies. Renew Sustain Energy Rev 2019;107:37–50. 10.1016/j.rser.2019.02.018.

[8] Bridgwater AV. Review of fast pyrolysis of biomass and product upgrading. Biomass Bioenergy 2012;38:68–94. 10.1016/j.biombioe.2011.01.048.

[9] Schmitt N, Apfelbacher A, Jäger N, Daschner R, Stenzel F, Hornung A. Thermochemical conversion of biomass and upgrading to biofuel: the thermo-catalytic reforming process – a review. Biofuels, Bioprod Biorefining 2019;13:822–37. doi:10.1002/bbb.1980.

[10] Valle B, Remiro A, García-Gómez N, Gayubo AG, Bilbao J. Recent research progress on bio-oil conversion into bio-fuels and raw chemicals: a review. J Chem Technol Biotechnol 2019;94:670–89. doi:10.1002/jctb.5758.

[11] Hornung A. Transformation of Biomass: Theory to Practice. Chichester: John Wiley & Sons Ltd; 2014. doi:101002/9781118693643.

[12] Elmously M, Jäger N, Apfelbacher A, Daschner R, Hornung A. Thermo-catalytic reforming of spent coffee grounds. Bioresour Bioprocess 2019;6:44. doi:10.1186/s40643-019-0281-5.

[13] Ouadi M, Jaeger N, Greenhalf C, Santos J, Conti R, Hornung A. Thermo-catalytic reforming of municipal solid waste. Waste Manag 2017;68:198–206. 10.1016/j.wasman.2017.06.044.

[14] Neumann J, Binder S, Apfelbacher A, Gasson JR, Ramírez García P, Hornung A. Production and characterization of a new quality pyrolysis oil, char and syngas from digestate – introducing the thermo-catalytic reforming process. J Anal Appl Pyrolysis 2015;113:137–42. 10.1016/j.jaap.2014.11.022.

[15] Lehto J, Oasmaa A, Solantausta Y, Kytö M, Chiaramonti D. Review of fuel oil quality and combustion of fast pyrolysis bio-oils from lignocellulosic biomass. Appl Energy 2014;116:178–90. 10.1016/j.apenergy.2013.11.040.

[16] Chiaramonti D, Oasmaa A, Solantausta Y. Power generation using fast pyrolysis liquids from biomass. Renew Sustain Energy Rev 2007;11:1056–86. 10.1016/j.rser.2005.07.008.

[17] Buffi M, Seljak T, Cappelletti A, Bettucci L, Valera-Medina A, Katrašnik T, et al. Performance and emissions of liquefied wood as fuel for a small scale gas turbine. Appl Energy 2018;230:1193–204. 10.1016/j.apenergy.2018.08.126.

[18] Chen J., Mitchell M.G., Nourse J.G. Development of ultra-low emission diesel fuel-fired microturbine engines for vehicular heavy duty applications: combustion modifications 2010:521–30. doi:10.1115/GT2010-23181.

[19] Chen J., Mitchell M.G., Nourse J.G. Development of ultra-low emission liquid fuel-fired microturbine engines for vehicular heavy duty applications 2009:281–9. doi:10.1115/GT2009-60257.

[20] Kislat O., Zanger J., Krummrein T., Kutne P., Aigner M. Detailed experimental investigation of the operational parameters of a 30 kW micro gas turbine 2019. doi:10.1115/GT2019-90709.

[21] Grimm F., Enderle B., Kislat O., Izadi S., Zanger J., Kutne P., et al. A re-design study based on a high pressure cyclonic combustor operated with liquid fuel 2019. doi:10.1115/GT2019-91528.

[22] Nakamura S, McDonell V, Samuelsen S. The effect of liquid-fuel preparation on gas turbine emissions. J Eng Gas Turbines Power 2008;130:21506–11.

[23] Zhang C, Xu Q, Lin Y, Zhu J, Yuan Y, Sung C-J. Experimental characterization of fuel-air mixing in a multihole tube. J Eng Gas Turbines Power 2012;134. doi:10.1115/1.4004437.

[24] Bolszo C., McDonell V., Samuelsen S. Impact of biodiesel on fuel preparation and emissions for a liquid fired gas turbine engine 2007:493–502. doi:10.1115/GT2007-27652.

[25] Bolszo CD, McDonell VG. Emissions optimization of a biodiesel fired gas turbine. Proc Combust Inst 2009;32:2949–56. 10.1016/j.proci.2008.07.042.

[26] Krishna C.R. Performance of the capstone C30 microturbine on biodiesel blends, BNL-77927-2007-IR. 2007.

[27] Nascimento MAR, Lora ES, Corrêa PSP, Andrade RV, Rendon MA, Venturini OJ, et al. Biodiesel fuel in diesel micro-turbine engines: modelling and experimental evaluation. Energy 2008;33:233–40. 10.1016/j.energy.2007.07.014.

[28] Prussi M, Chiaramonti D, Riccio G, Martelli F, Pari L. Straight vegetable oil use in micro-gas turbines: system adaptation and testing. Appl Energy 2012;89:287–95. 10.1016/j.apenergy.2011.07.031.

[29] Chiariello F, Allouis C, Reale F, Massoli P. Gaseous and particulate emissions of a micro gas turbine fuelled by straight vegetable oil–kerosene blends. Exp Therm Fluid Sci 2014;56:16–22. 10.1016/j.expthermflusci.2013.11.013.

[30] Kun-Balog A, Sztankó K. Reduction of pollutant emissions from a rapeseed oil fired micro gas turbine burner. Fuel Process Technol 2015;134:352–9. 10.1016/j.fuproc.2015.02.017.

[31] Shaddix C.R., Hardesty D.R. Combustion properties of biomass flash pyrolisis oils: final project report (SAND99-8238). 1999. doi:10.2172/5983.

[32] Oasmaa A, Kytö M, Sipilä K. Pyrolysis oil combustion tests in an industrial boiler. Prog. Thermochem. Biomass Convers. 2001:1468–81 Wiley Online Library.

[33] Broumand M, Shahzeb Khan M, Yun S, Hong Z, Thomson MJ. The role of atomization in the spray combustion of a fast pyrolysis bio-oil. Fuel 2020;276:118035. 10.1016/j.fuel.2020.118035.

[34] Zadmajid S, Albert-Green S, Afarin Y, Thomson MJ. Optimizing a swirl burner for pyrolysis liquid biofuel (Bio-oil) combustion without blending. Energy Fuels 2017;31:6065–79. doi:10.1021/acs.energyfuels.6b03417.

[35] Albert-Green S, Thomson MJ. The effects of nozzle design on the combustion of wood-derived fast pyrolysis oil. Biomass Bioenergy 2018;117:102–14. 10.1016/j.biombioe.2018.07.002.

[36] Conti R, Jäger N, Neumann J, Apfelbacher A, Daschner R, Hornung A. Thermocatalytic reforming of biomass waste streams. Energy Technol 2017;5:104–10. doi:10.1002/ente.201600168.

[37] Neumann J, Hornung A, Apfelbacher A, Daschner R. Pyrolysis of residual biomass via themo-catalytic reforming- experimental investigation of sewage sludge. In: Proceedings of the 25th European biomass conference and exhibition stock; 2017. p. 949–51.

[38] Tzanetakis T, Ashgriz N, James DF, Thomson MJ. Liquid fuel properties of a hardwood-derived bio-oil fraction. Energy Fuels 2008;22:2725–33. doi:10.1021/ef7007425.

[39] Lefebvre A, McDonell V. Atomization and Sprays. 2nd ed. Boca Raton: CRC Press; 2017.

[40] Lefebvre AH, Ballal DR. Gas Turbine Combustion - Alternative Fuels and Emissions. 3rd ed. FL, USA: CRC Press (Taylor Frances Group); 2010.

[41] D'Alessio J, Lazzaro M, Massoli P, Moccia V. Thermo-optical investigation of burning biomass pyrolysis oil droplets. Symp Combust 1998;27:1915–22. 10.1016/S0082-0784(98)80035-0.

[42] Varga CM, Lasheras JC, Hopfinger EJ. Initial breakup of a small-diameter liquid jet by a high-speed gas stream. J Fluid Mech 2003;497:405–34. doi:10.1017/S0022112003006724.

[43] Lefebvre AH. Energy Considerations in Twin-Fluid Atomization. J Eng Gas Turbines Power 1992;114:89–96.

[44] Moloodi S, Tzanetakis T, Nguyen B, Zarghami-Tehran M, Khan U, Thomson MJ. Fuel property effects on the combustion performance and emissions of hardwood-derived fast pyrolysis liquid-ethanol blends in a swirl burner. Energy Fuels 2012;26:5452–61. doi:10.1021/ef300657d.

[45] Zeldovich YB. The oxidation of nitrogen in combustion explosions. Acta Physicochim USSR 1946;21:577–628.

[46] Fenimore CP. Formation of nitric oxide in premixed hydrocarbon flames. Symp Combust 1971;13:373–80. 10.1016/S0082-0784(71)80040-1.